Characterization of the Oligomeric States of Insulin in Self-Assembly and Amyloid Fibril Formation by Mass Spectrometry

Ewan J. Nettleton,* Paula Tito,* Margaret Sunde,† Mario Bouchard,* Christopher M. Dobson,* and Carol V. Robinson*

*Oxford Centre for Molecular Sciences, New Chemistry Laboratory, University of Oxford, Oxford, OX1 3QT, and †Department of Biochemistry, University of Cambridge, Old Addenbrooke's Site, Cambridge, CB2 1GA, United Kingdom

ABSTRACT The self-assembly and aggregation of insulin molecules has been investigated by means of nanoflow electrospray mass spectrometry. Hexamers of insulin containing predominantly two, but up to four, Zn^{2+} ions were observed in the gas phase when solutions at pH 4.0 were examined. At pH 3.3, in the absence of Zn^{2+}, dimers and tetramers are observed. Spectra obtained from solutions of insulin at millimolar concentrations at pH 2.0, conditions under which insulin is known to aggregate in solution, showed signals from a range of higher oligomers. Clusters containing up to 12 molecules could be detected in the gas phase. Hydrogen exchange measurements show that in solution these higher oligomers are in rapid equilibrium with monomeric insulin. At elevated temperatures, under conditions where insulin rapidly forms amyloid fibrils, the concentration of soluble higher oligomers was found to decrease with time yielding insoluble high molecular weight aggregates and then fibrils. The fibrils formed were examined by electron microscopy and the results show that the amorphous aggregates formed initially are converted to twisted, unbranched fibrils containing several protofilaments. Fourier transform infrared spectroscopy shows that both the soluble form of insulin and the initial aggregates are predominantly helical, but that formation of β-sheet structure occurs simultaneously with the appearance of well-defined fibrils.

INTRODUCTION

Mass spectrometry (MS) is undergoing a period of unprecedented growth in its applications. This is due largely to its wide spread use in sequencing for proteomic applications (Kuster and Mann, 1998), but also to the growing number of examples of non-covalent interactions that have been maintained in the gas phase (Rostom and Robinson, 1999). The growth in both these applications derives largely from technological advances, particularly the introduction of nanoflow electrospray techniques (Wilm and Mann, 1994). This methodology has lead to an enhanced sensitivity, important for proteomic applications, and facilitated the analysis of aqueous solutions containing metal ions and buffers (Vis et al., 1998); this is critical for the study of non-covalent interactions. In addition the recent combination of nanoflow electrospray with time-of-flight analysis offers the promise of an unlimited mass-to-charge range, a property that is only beginning to be realized and which has enabled the analysis of intact ribosomes (Rostom et al., 2000) and viruses (Tito et al., 2000). These observations of multi-protein complexes suggest that it may now be possible to apply mass spectrometry to study large, weakly associated protein aggregates in solution. The process of aggregation is notoriously difficult to study directly by conventional techniques but is becoming increasingly important for example as it is widely accepted to be involved in the early stages of amyloid fibril formation (Harper and Lansbury, 1997). Insulin provides an ideal system for testing this hypothesis since it forms well-defined oligomers in its native state yet can be induced to aggregate and form amyloid fibrils under non-physiological conditions. Consequently insulin can form both specific and nonspecific oligomeric states, providing an excellent model system for distinguishing such associations by mass spectrometry. Moreover understanding the aggregation process is important, not only in this case from the point of view of the long-term storage and pharmaceutical use of insulin, but also for the possible insight it may provide into the mechanism of protein aggregation and fibril formation more generally.

The protein hormone insulin is synthesized in the β cells of the pancreas where it is stored as a Zn^{2+}-containing hexamer. X-ray analysis of the two Zn^{2+} hexamers of porcine insulin shows that each monomer unit is essentially helical and contains 51 amino acids in two chains (an acidic A chain of 21 residues and a basic B chain of 30 residues), cross-linked by two disulfide bridges (Adams et al., 1969). A third disulfide bridge links two parts of the A chain. The two-Zn^{2+} hexamer is composed of three equivalent dimers, each coordinated by the side chains of B10 His. In the treatment of type I diabetes the Zn^{2+}-containing hexamer of insulin is injected into the musculature. Its large size, however, prevents its efficient absorption into the blood stream. Hexamers are therefore broken down to dimers and then monomers that are then transported efficiently into the blood stream (Brange et al., 1997c). Both the monomeric and dimeric forms of insulin are prone to aggregation, a property that has severely limited the use of insulin in pharmaceutical preparations. The formation of aggregation-prone species is avoided during storage and injection of insulin by the use of the more stable two-Zn^{2+} hexamer

Received for publication 6 March 2000 and in final form 4 May 2000.

Address reprint requests to Dr. Carol V. Robinson, University of Oxford, New Chemistry Laboratory, South Parks Rd., Oxford, OX1 3 QT, UK. Tel.: 44-1865-275981; Fax: 44-1865-275948; E-mail: carolr@bioch.ox.ac.uk.

0006-3495/00/08/1053/13 $2.00

(Brange et al., 1997c) or by the use of analogs of insulin that are stable in monomeric form (Brange and Volund, 1999).

In addition to forming well-defined assemblies under native conditions insulin has been found to form amyloid fibrils in vitro (Langmuir and Waugh, 1940). The turbidity of solutions was used to indicate the extent of the aggregation process and was shown to be more rapid at high temperatures (60–70°C), at low pH (1.5–2.0) and at relatively high protein concentrations (mM) (Brange et al., 1997a). Early x-ray diffraction patterns of in vitro insulin fibrils formed under these conditions were interpreted as showing an essentially linear aggregate of slightly modified native insulin (Koltun et al., 1954). Later studies, however, using x-ray diffraction in combination with optical spectroscopy proposed that substantial changes in conformation accompany the formation of cross-β-fibrils from native insulin (Burke and Rougvie, 1972b). In vitro studies have shown that removal of residues at the C-terminus of the B chain, to give the des-pentapeptide and des-octapeptide species, leads to an increased rate of aggregation while linking the C-terminus of the B chain to the N-terminus of the A chain leads to a greatly reduced tendency to form aggregates (Brange et al., 1997a). These findings have been interpreted to imply that the C-terminus plays a major role in the process of fibril formation. A model based on the crystal structure of despentapepetide insulin was used to suggest that insulin enters the fibril with little perturbation from the helical structure of the native state (Brange et al., 1997b). Infrared spectroscopy, however, indicates that significant conversion of α-helical to β-sheet structure accompanies formation of amyloid fibrils (Burke and Rougvie, 1972a; Bouchard et al., submitted).

In this paper we describe the use of a nanoflow electrospray (nano-ES) mass spectrometric approach to probe the nature of the species present in solution when bovine insulin undergoes self-assembly, aggregation and amyloid fibril formation. Using carefully controlled nano-ES mass spectrometry conditions we have monitored the formation of soluble oligomers of the insulin molecule in its native conformation. Under conditions that promote more extensive aggregation we have probed the association of oligomers using time-of-flight mass analysis. Using hydrogen exchange methods, we have examined the equilibrium between monomeric and oligomeric forms of the protein. Under the same solution conditions, but at elevated temperatures, the conversion of these soluble oligomers to amyloid fibrils appears more rapid and the presence of the various oligomers is explored as a function of time. To verify that fibrils form during these experiments the solutions were examined by electron microscopy, x-ray diffraction and Fourier transform infrared spectroscopy (FT-IR). Combination of the mass spectrometry data together with the FT-IR suggests an outline of the structural transitions involved in the formation of amyloid fibrils from soluble insulin molecules.

MATERIALS AND METHODS

Materials

Bovine and human insulins were purchased from Sigma Chemical Company (Poole, Dorset, UK). MilliQ water (Millipore Ltd., Bedford, MA) was used in all experiments and the pH of buffers was adjusted using HCl (Fisons Scientific, Loughborough, UK) or ammonia (BDH, Poole, UK). Zinc phosphate was purchased from Sigma Chemical Company (Poole, Dorset, UK). The concentration of protein solutions was determined by the Bicinchoninic acid assay (Pierce Chemical Company, Rockford, IL). D_2O and DCl were purchased from Aldrich Chemical Co, Poole, Dorset, and Fluka, Buchs, Switzerland, respectively.

Mass spectrometry

All mass spectra were recorded on Platform II and Q-tof mass spectrometers (Micromass UK Ltd.) without source heating and in the absence of organic co-solvents. 2 μl of protein solution were introduced via a nanoflow electrospray interface from a gold-plated borosilicate needle with approximately 1 μm internal diameter at 20°C. Needles were prepared in house from borosilicate glass capillaries (Clarke Electromedical Instruments, Reading, UK) of external diameter 1.0 mm and internal diameter 0.5 mm on a model P-97 Flaming/Brown micropipette puller (Sutter Instrument Company, Sittingbourne, UK), and gold coated with a Polaron SEM coating system (Applied Vacuum Engineers, Bristol, UK). Mass spectrometer conditions were set with a capillary voltage of 1.3 kV and a skimmer offset of 5 V and a source pressure of 5×10^{-5} mBar with the use of a collision gas in the Q-tof mass spectrometer to achieve this pressure. Each spectrum was obtained from a new aliquot of the protein solution and a new nanoflow needle was used for each acquisition. Analysis of the mass spectra was performed with MassLynx 3.1, (Micromass UK Ltd.). The average masses of protein samples were calculated from the charge states shown. All spectra were calibrated using hen lysozyme (Sigma Chemical Co., Poole, Dorset, UK) in H_2O at pH 5.0. The masses measured are centroid values, which take into account the asymmetry of the peaks arising from the natural isotope distribution. The estimated error in these measurements is calculated from the standard deviation of the charge states. All mass spectra are presented as raw data, on a *m/z* scale, with minimal smoothing and without any resolution enhancement. The data were acquired in triplicate to confirm the reproducibility of the results. Desalted samples were prepared by washing extensively on Centricon 3 concentrators (Amicon, Stonehouse, Gloucestershire, UK) with H_2O at pH 2.0 to give a stock solution with a concentration of approximately 30 mg/ml. Insulin samples at pH 2.0 and at various protein concentrations were prepared by dilution of the stock solution into a HCl buffer at pH 2.0. Samples at pH 3.3 and pH 4.0 were prepared by further dialysis of the stock solution using Centricon 3 concentrators with an HCl buffer at the appropriate pH. Samples at pH 4.0, containing excess Zn^{2+} as the only metal ion present, were prepared by further washing of the pH 2.0 protein stock solutions with a HCl buffer at pH 4.0 containing 10 mM zinc phosphate. The concentration of soluble bovine protein during the aggregation process was measured using an equimolar quantity human insulin as an internal standard. An aliquot of the human protein (5 μl) was added immediately prior to recording the spectrum to a 5 μl aliquot of the pH 2.0 solution incubated at 70°C for various times. This allows the relative intensities of the two protein signals to be recorded in the same spectrum and provides a measure of the concentration of the soluble bovine protein.

FT-IR

For FT-IR analyses insulin was dissolved in D_2O and the solution was adjusted to pH* (glass electrode pH reading in D_2O solution) 2.0 with DCl (Fluka, Buchs, Switzerland). Deuterated-protein samples were prepared by

dissolving protein in 10 ml of the D_2O buffer to give a solution of 10 mg/ml. After 24 h the sample was lyophilized and this procedure was repeated until mass spectrometry analysis showed that all exchange-labile protons in the protein had exchanged with deuterons. The mass spectrum of this sample gave a mass of 5818 Da consistent with >98% deuterium incorporation. Infrared spectra of protein samples mounted between two NaCl plates were collected on a FT-IR spectrometer (BioRad). Soluble deuterated-protein samples were analyzed at ~20 mg/ml in D_2O at pH* 2.0, while fibril samples were analyzed as a suspension in the same buffer.

Electron microscopy

Fibril formation was followed for both deuterated and non-deuterated protein solution in D_2O and H_2O at 0.2 mM protein concentration, pH* 2.0 (with HCl). This solution was incubated at 70°C for between 3 and 48 h. Samples for electron microscopy were prepared for analysis on Formvar-coated grids negatively stained with 2% (wt/vol) uranyl acetate in water, washed, air dried, and then analyzed in a JEOL JEM1010 transmission electron microscope operating at an accelerating voltage of 80 kV.

RESULTS

Mass spectrometry of specific assemblies of insulin

Insulin solutions at 2 mM protein concentration and pH 4.0 in the presence of excess Zn^{2+} and Cl^- ions were analyzed by nano-ES MS. The spectra show a series of peaks corresponding to different charge states of the protein. These states arise from the electrospray process, and the number of charges is related to the number of accessible basic sites on the protein molecules (Mirza and Chait, 1994). The predominant charge states (approximately 90% of the total ion intensity) lie between *m/z* 2800 and 4000 (Fig. 1). These are assigned to +9, +10, and +11 and correspond to a molecular mass of 34.528 ± 7 Da, a value in close agreement with that calculated (35532 Da) for a hexamer of insulin with two Zn^{2+} ions bound (Table 1). In addition, charge states of monomeric (~8%) and dimeric species (<1%) can also be detected in the spectra. The proportions of the oligomers, calculated from the area under the peaks enables the value of the association constant (K_A) of dimer to hexamer to be calculated as $1.49 \pm 0.2 \times 10^{10}$ M at pH 4.0. This value is in reasonable agreement with a value determined from solution measurements under somewhat different conditions (4.0×10^8 M) (Goldman and Carpenter, 1974). Both methods reflect the highly favorable association constant for the formation of the hexamer in the presence of Zn^{2+}.

Closer examination of individual charge states of the hexameric complex indicates that they consist of not one but a number of well-defined peaks (Fig. 1). The masses measured from these peaks identify them as arising from insulin hexamers differing in the number of bound Zn^{2+} ions (Table 1). The most abundant hexameric species observed by MS has two bound Zn^{2+} ions but there are also intense peaks corresponding to hexamer assemblies containing three and four Zn^{2+} ions. Previous mass spectrometry measurements established that Zn^{2+} bound hexamers could be maintained in the gas phase from analysis of a solution at pH 8.0 and the heterogeneity observed in the spectrum was attributed to the binding of water molecules (Fabris and Fenneslau, 1999). Analysis of x-ray structures has shown hexamer assemblies with two further sites for Zn^{2+} binding in addition to the two major sites (Schlichtkrull, 1958). More recent x-ray studies have shown that even in the presence of excess Zn^{2+}, these two additional sites are not completely occupied in the crystal (Smith et al., 1984), resulting in partial occupancy of four Zn^{2+} sites and giving a Zn^{2+} content on average between two and three Zn^{2+} ions

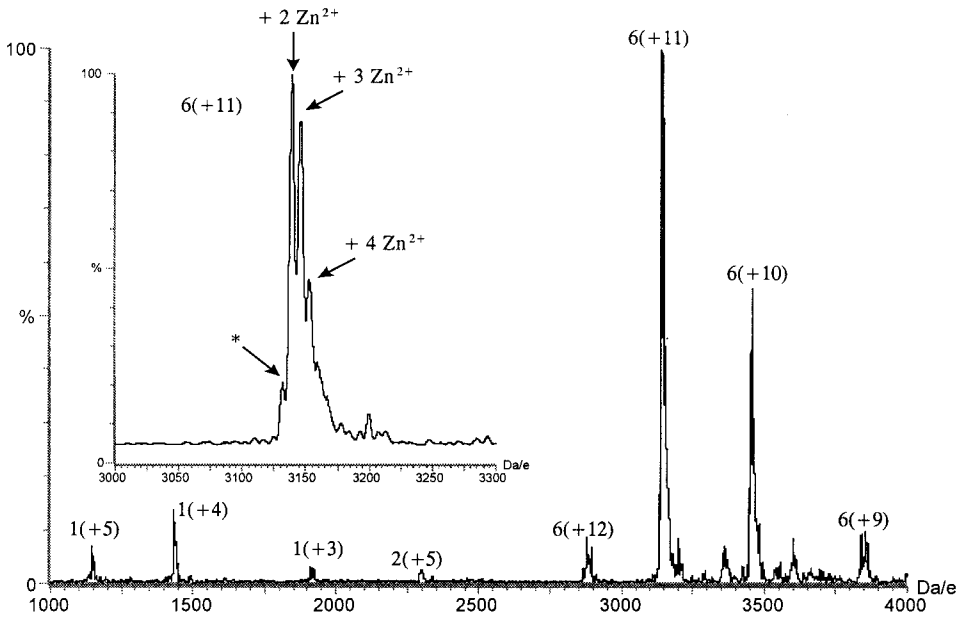

FIGURE 1 Nano-ES mass spectrum of insulin at pH 4.0 in the presence of Zn^{2+} and Cl^- ions showing that the dominant charge states (+11 and +10) correspond in mass to the hexamer with a small proportion of monomer and dimer present, The number of insulin molecules in the oligomer is indicated and the charge state is shown in parentheses. *Inset:* Expansion of the +11 charge state of the hexamer showing that the major species contains two bound Zn^{2+} ions but species containing up to four Zn^{2+} ions are observed. There is an additional low intensity species at *m/z* 2458 (labeled *), which corresponds in mass to a two-Zn^{2+} hexamer in which one insulin molecule contains a C-terminal alanine truncation. Although this impurity is present in monomeric forms of insulin (~1–2%), in the hexamer the probability of one of the six insulin molecules containing this truncation is increased.

TABLE 1 Calculated and measured masses for insulin in the presence and absence of Zn^{2+} and in the oligomeric forms observed at pH 3.2 and pH 2.0

Species	No. of Zn^{2+}	Charge states	Calculated mass (Da)	Measured mass (Da)
Monomer	0	+3 to +6	5,734	5,733 ± 1
Dimer	0	+6 to +8	11,467	11,466 ± 2
Trimer	0	+8	17,201	17,198
Tetramer	0	+8 to +10	22,932	22,932 ± 0.1
Pentamer	0	+7 to +9	28,665	28,666 ± 0.5
Hexamer	0	+8 to +10	34,398	34,399 ± 0.1
Hexamer*	2	+9 to +12	34,461	34,464 ± 8
Hexamer	2	+9 to +12	34,532	34,528 ± 7
Hexamer	3	+9 to +12	34,598	34,598 ± 10
Hexamer	4	+9 to +12	34,663	34,666 ± 8
7-Mer	0	+9 to +11	40,131	40,146 ± 12
8-Mer	0	+10 to +12	45,864	45,870 ± 11
9-Mer	0	+11 to +13	51,597	51,613 ± 8
10-Mer	0	+12, +13	57,330	57,344 ± 3
11-Mer	0	+13, +14	63,063	63,154 ± 9
12-Mer	0	+14	68,796	68,832

*This species arises from the assembly of five full-length insulin molecules and a small proportion of truncated insulin (~2%).

per hexamer. Hexameric species with more than four, or less than two, Zn^{2+} ions bound were not detected indicating that the binding of zinc in this assembly is specific. Consequently the number of Zn^{2+} ions in hexamers observed by MS agrees very well with the occupancy anticipated from crystallographic experiments.

Concentration-dependent association of insulin has been observed in solution in the absence of Zn^{2+} (Jeffrey and Coates, 1966; Lord et al., 1973; Pocker and Biswas, 1981). This is also evident in mass spectra of insulin obtained from solutions at pH 3.3 over the concentration range 2 μ M to 5 mM (Fig. 2). At a protein concentration of 2 μM, charge states of +4 and +5 are observed at high intensity and their masses confirm that they arise from monomeric insulin (Table 1). Increasing the concentration of insulin to 10 μM gives rise to an additional peak, just visible in the spectrum of the protein at a concentration of 2 μM. This peak can be assigned to the +7 charge state of the insulin dimer. Since the even numbered charge states of the dimer will occur at the same *m/z* values as those of the monomer, observation of an odd numbered charge state, such as +7, is necessary to identify the presence of dimeric insulin in the gas phase (Table 1). It is interesting to note that at pH 3.3, where the majority of side chains are positively charged, the dominant charge states for the monomer and dimer are +5 and +7, respectively. This reduction from 10 to 7 charges for a pair of molecular ions when forming a dimer suggests that at, on average, three ionic interactions not present in the monomeric species are involved in the stabilization of the dimer structure.

As the concentration of the insulin solution is increased from 10 μM to 200 μM there is a large increase in the intensity of the +7 charge state, an observation consistent with increased dimer formation at higher protein concentrations. At insulin concentrations of 1 mM and 5 mM, additional peaks in the range *m/z* 2000–2900 are evident. These arise predominantly from the charge states of a single additional species, a tetramer (Table 1). For the reasons outlined above, the +9 charge state provides a unique assignment for the tetramer. Measurement of the relative proportions of the species detected at the different protein concentrations enables the estimation of association constants. A plot of the fractional intensity of the peaks assigned to dimeric species present in mass spectra against the concentration of insulin measured over the range from 2 μM to 200 μM, enables K_{12} to be determined as 1.0×10^4 M (Fig. 2 *B*). This value is similar to reported values of 0.75×10^4 M, measured at pH 3.5 and 26°C, and 1.09×10^4 M, measured at pH 2.0 and 15°C for K_{12} (Lord et al., 1973). For the solution conditions used here, pH 3.3 and 22°C, K_{24} was found to be $7.7 \pm 1.8 \times 10^1$ M. The reported values of K_{24} at pH 7.0 and pH 2.0 are 5×10^3 M and 7.8×10^2 M, respectively (Pocker and Biswas, 1981; Jeffrey and Coates, 1966). The value determined by MS for K_{24} is lower than those reported for solution based measurements at pH 2.0 and 7.0. This may arise from the different solution conditions employed for the measurements. Nevertheless all three measurements indicate that dimer to tetramer association is very weak and is therefore likely to be prone to error. The value determined by MS for K_{12}, however, is more favorable and is very similar to that determined from solution based methods.

Mass spectrometry of insulin under aggregation conditions

The spectrum of a 2 mM solution of insulin at pH 2.0 is highly complex with multiple series of charge states in the *m/z* range 3800–5000 (Fig. 3). The latter can be assigned to assemblies containing up to 12 molecules of insulin. The analysis of these data is, however, complicated since several oligomers give rise to overlapping charge states. In order to overcome this problem, the charge states of all oligomers from a tetramer to a 12-mer were simulated. Using this procedure the +9 and +11 charge states of the 7-mer can be assigned uniquely (Fig. 3 and Table 1), since no other oligomers are predicted to give rise to significant intensity at these *m/z* values (4460 and 3649, respectively). The peak at *m/z* 4300, by contrast, could arise from three different species, a hexamer (+8), a 9-mer (+12), or a 12-mer (+16). Since the electrospray process produces a distribution of charges on the oligomeric species, giving rise to a charge state distribution that rarely contains less than three charge states with significant intensity, the absence of detectable signals from neighboring charge states can be used to distinguish these possibilities. For example, the 9-mer charge states (+11) and (+13) have unique assignments at *m/z*

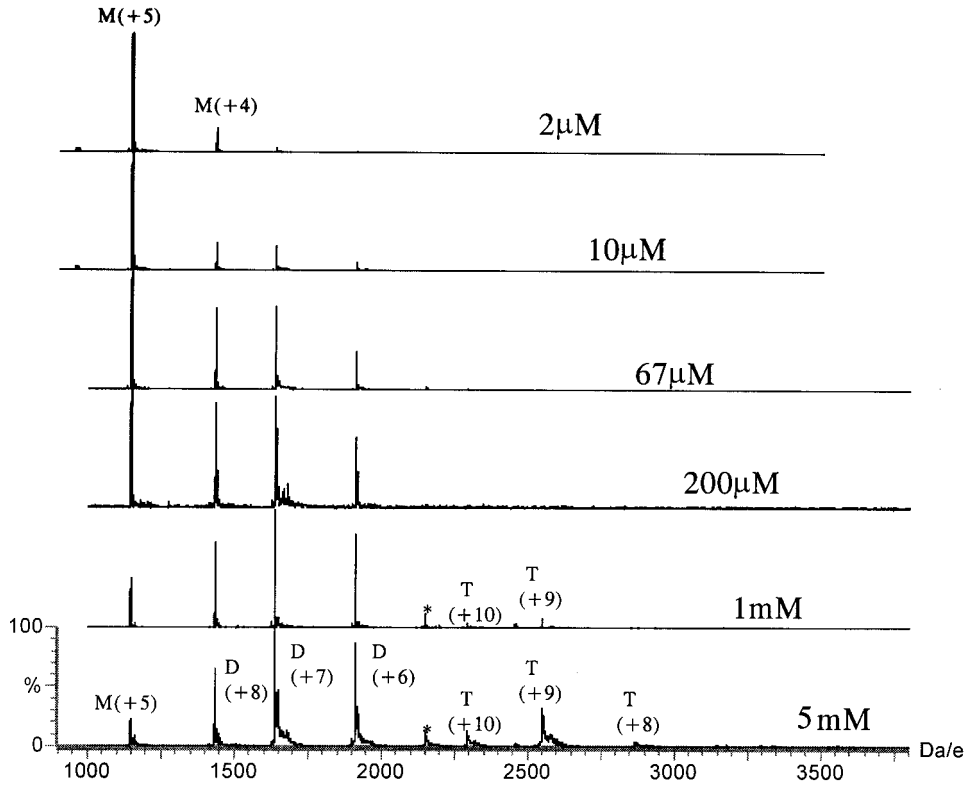

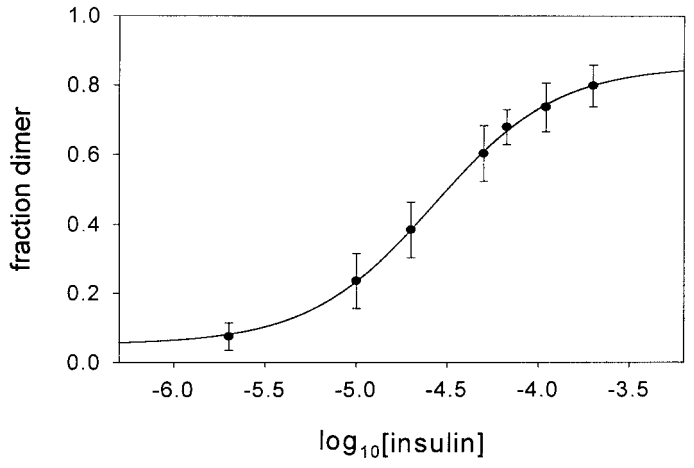

FIGURE 2 (*A*) Nano-ES mass spectra of insulin at pH 3.3 over the concentration range 2 μM to 5 mM. The charge states labeled M, D, and T represent monomeric, dimeric, and tetrameric insulin. The number in parentheses is the charge on the ion. The peaks labeled * in the spectra obtained from the 1 and 5 mM insulin solutions are assigned to the +7 charge state of trimeric insulin. The presence of this trimer has not been reported in solution and is probably an intermediate in the disassembly of the weakly associated tetramer in the gas phase. (*B*) Plot of the fraction of the dimer observed by MS against the logarithm of the insulin concentration in the range 2–200 μM at pH 3.3 and 22°C. The fraction of dimer was calculated by summing the peaks assigned to the dimer and expressing this value as a fraction of the total signal intensity. Error bars were estimated from the differences in the intensities of the peak in replicate experiments.

4691 and 3969, while the (+14) charge state of the 12-mer is identified at *m/z* 4915. The low intensities of the signals observed for the 9-mer (+11 and +13) and the 12-mer (+14), and the intense peak assigned to the hexamer (+9), indicate that the major contribution to the peak at *m/z* 4300 is from the hexamer (+8). Using this approach the complete spectrum can be assigned (Fig. 3). It is interesting to note that although the absolute intensities are sensitive to the mass spectrometry conditions, the relative intensities of different oligomers are reproducible and indicate that some oligomers are present at higher concentrations than others. Moreover, the distribution of the oligomers is almost identical whether or not buffer salts are present (data not shown). For example, the charge states for the hexamer are

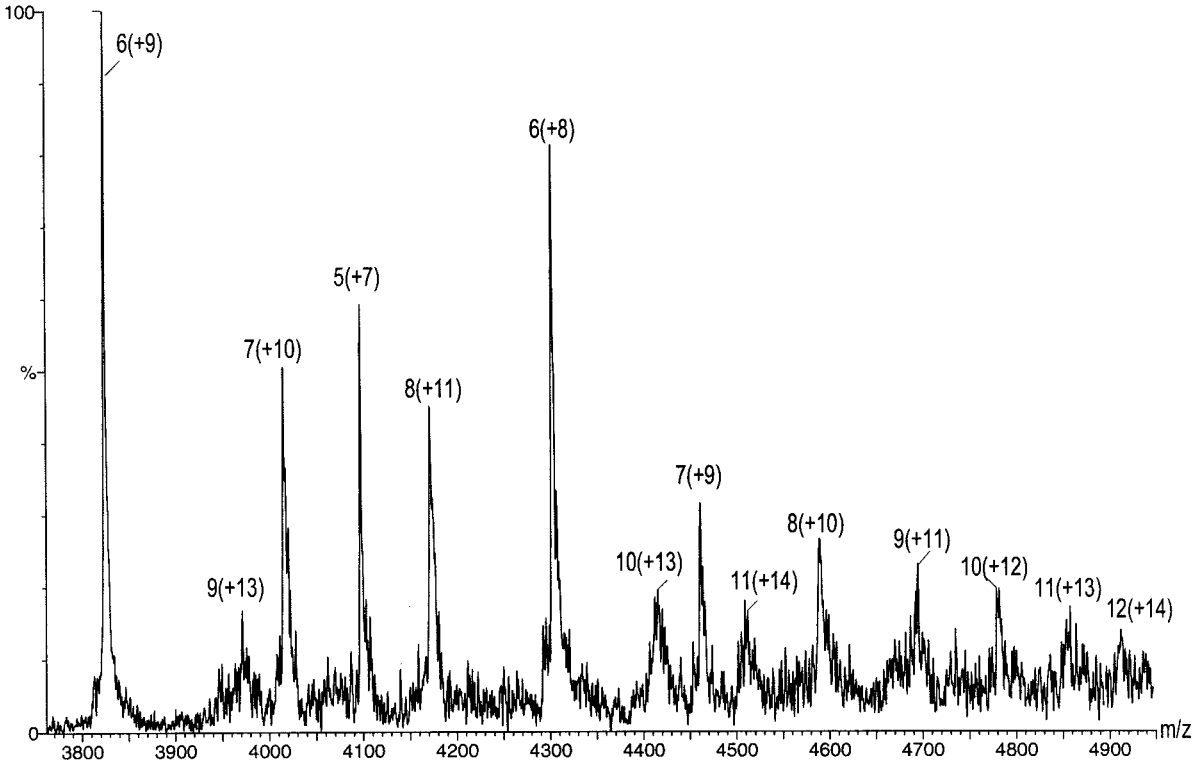

FIGURE 3 Nano-ES mass spectrum from *m/z* 3700 to 5000 showing populations of higher oligomers present at pH 2.0, 2 mM, and 22°C. The number of molecules in the oligomer is indicated and the charge state is shown in parentheses.

always more intense that those for the pentamer and 7-mer indicating that it is present at greater abundance. This suggests that the hexamer has a higher intrinsic stability than the pentamer and 7-mer.

In order to investigate the dynamic structure of the oligomeric species we have used hydrogen exchange methods to measure solvent exchange of labile hydrogens in oligomers containing from two to six insulin molecules. The nano-ES mass spectra of the trimer, tetramer, pentamer, and hexamer of insulin before and after 1 h of exposure to D_2O are shown in Fig. 4 *A*. These show that the absolute increase in mass observed in D_2O solution is greater for higher oligomers than for lower ones. Using this procedure the hydrogen exchange kinetics of oligomers were monitored over a time course from 10 min to 24 h and the results plotted in Fig. 6 *B*. The results show that the hydrogen exchange profiles are remarkably similar, a result consistent with a linear increase in the number of sites protected as the number of molecules in the oligomers increases. An alternative model is that increased size of the oligomers leads to an exponential increase in protection. This is clearly not observed under the conditions of this experiment. Calculation of the number of slowly exchanging sites per insulin molecule after 360 min gives 20 ± 2, 20 ± 2, and 21 ± 4 for the dimer, tetramer, and hexamer respectively. These results indicate therefore that the molecular units in the various oligomers have approximately equal protection against exchange.

The possible role of these oligomers in fibril formation was investigated by monitoring the concentrations of the various species in solution at pH 2.0 and at a temperature of 70°C, conditions shown previously to promote fibril formation (Waugh et al., 1957; Brange et al., 1997a). Under these conditions the solutions become increasingly difficult to spray due to the presence of insoluble material in the nanoflow needle tip. In order to measure the concentration of the soluble bovine protein more accurately, human insulin was added as an internal standard immediately before analysis. This protein has the same ionization efficiency as the bovine protein and does not form aggregates on the time scale and conditions of the analysis (see Methods). The results show that during the first ~1 h of exposure to the fibril forming conditions, the total area under the peak assigned to bovine insulin does not change with respect to the internal standard (Fig. 5, *inset*). At longer times a steady decrease in relative intensity of the peaks assigned to bovine insulin was observed. After 2.5 h the bovine protein could not be measured relative to the peaks of the internal standard indicating that the protein is in a highly aggregated structure. These data show that there is a lag time for fibril formation; this was determined to be 65 ± 5 min under the conditions used here for a 2 mM solution. Spectroscopic data for a solution with

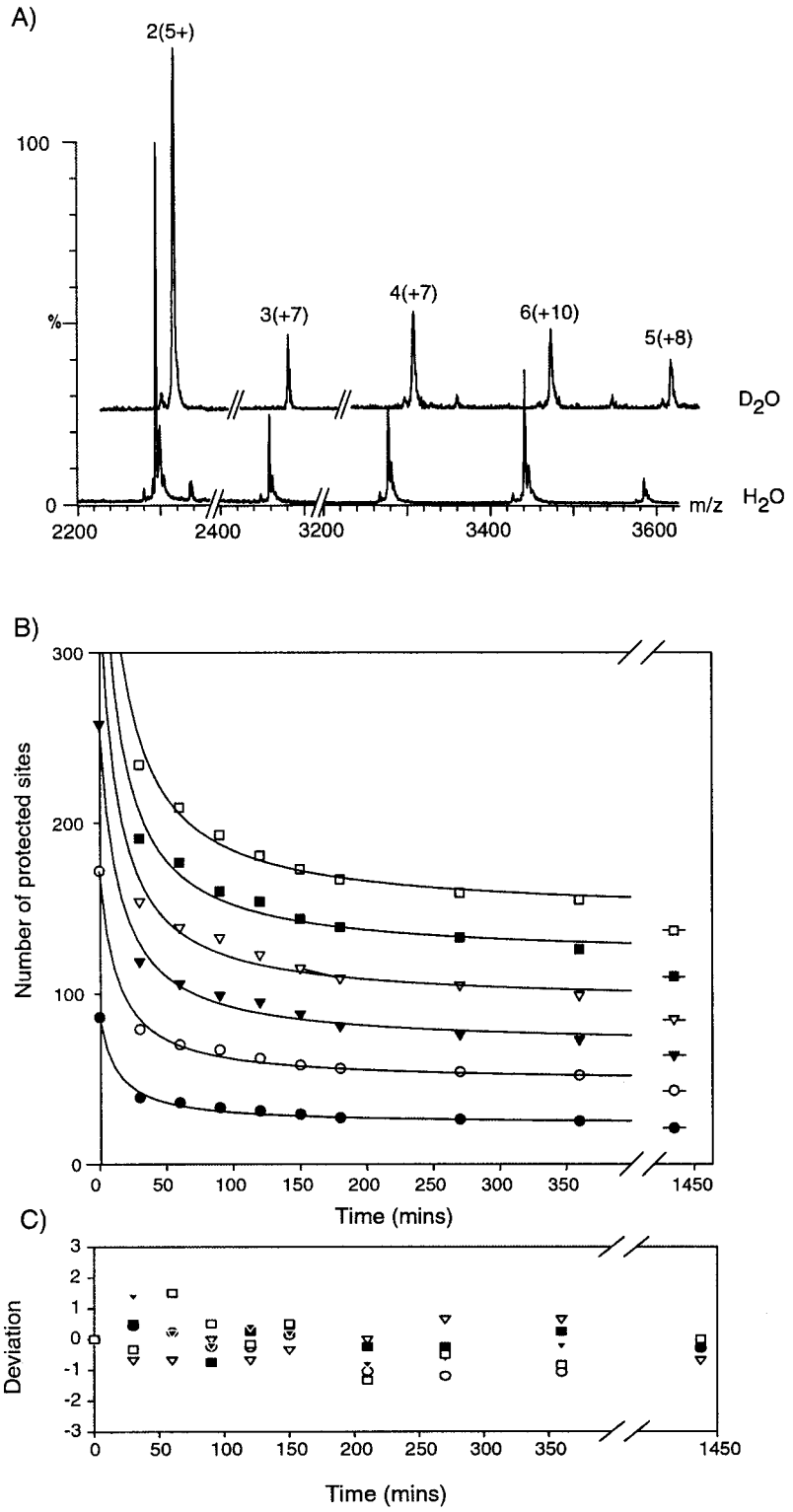

FIGURE 4 Hydrogen exchange of oligomers formed under aggregation conditions at pH 2.0, 2 mM and room temperature. (*A*) Mass spectra of oligomers formed in H_2O and after 1 h in D_2O. (*B*) Plot of the number of protected sites remaining in (●), dimeric (○), trimeric (▼), tetrameric (▽), pentameric (■), and hexameric (□) insulin species as a function of time. (*C*) Plot of the deviation of the hydrogen exchange protection of the oligomers from that observed for monomeric insulin. This value was calculated by dividing the total hydrogen exchange protection measured for each oligomer by the number of insulin molecules in each species.

a protein concentration of 8.8 mM at pH 1.55 at 80°C has shown previously that fibrils began to form after approximately 50 min (Waugh et al., 1957). These data therefore appear to be reasonably consistent despite the different solution conditions. For solutions of 200 μM and 20 μM protein at 70°C, lag times of 120 $\pm$ 10 min and more than 6 h, respectively, were obtained using the mass spectrometric approach.

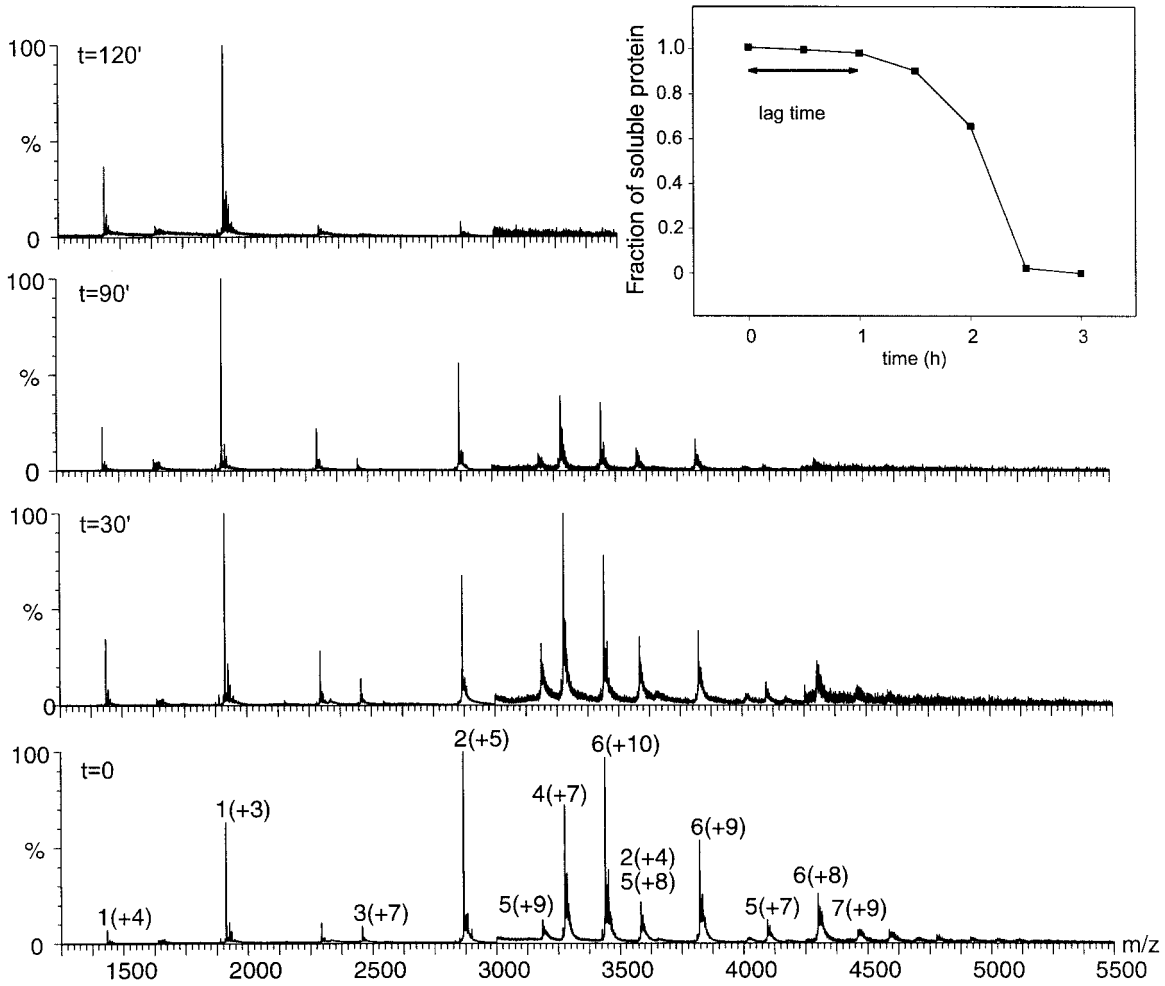

FIGURE 5 Insert: Plot of the concentration of soluble insulin measured indirectly by the decrease in the charge states in the mass spectrum of insulin relative to an internal standard against time (see Experimental Procedures). After 65 min the concentration decreases rapidly indicating rapid depletion of soluble insulin as large aggregates form. Nano-ES mass spectra of insulin at 2 mM concentration after incubation at 70°C and pH 2.0. At $t = 0$, before heating, the mass spectrum shows predominantly monomeric and dimeric insulin with lower proportions of tetramer, pentamer and hexamer. After heating for 30 min at 70°C the intensity of the hexamer and tetramer charge states are reduced relative to those of the pentamer. After 1.5 h the presence of higher oligomers is significantly reduced and after 2 h monomeric insulin is the only species that can be observed in the mass spectrum. The spectrum above *m/z* 3000 has been multiplied by a factor of 40 to enable observation of the oligomers.

The distribution of the various oligomers present in the insulin solution, shown in Fig. 5, was monitored as a function of time during the aggregation process. Although this process is extremely sensitive to the experimental conditions, reproducible results could be obtained under carefully controlled conditions. At the start of the time course the spectrum recorded corresponds predominately to that of monomeric and dimeric insulin although in the *m/z* range between 3000 and 5000, it is possible to observe oligomeric species similar to those shown in Fig. 3. The most intense signals in this range are assigned as described above to a tetramer (+7), pentamer (+7, +8, +9), hexamer (+10, +9, +8), and 7-mer (+9, +10). These assignments enable the relative proportions of the different species under aggregation conditions to be monitored with time. After 0.5 h at 70°C and pH 2.0 the relative intensities of all the oligomeric species are seen to decrease markedly and the relative proportion of hexamer has decreased more markedly than that of the tetramer and pentamer. After 2 h the signals from the higher oligomers are only just visible and the intensities of the charge states from monomeric species are reduced significantly. The dimer (+5) peak is also significantly reduced relative to those of the other oligomers and the monomer (+3). These observations could be a result of changes in the total concentration of insulin in solution or could reflect the reduced stability of the various oligomers relative to the monomer at higher temperatures. In order to address the latter possibility, the time-dependence experiments were repeated at 60°C. At this temperature, where aggregation does not take place at a detectable rate, the

relative proportions of the hexamer to the tetramer, pentamer and 7-mer did not change over the 2 h time course of the experiment. These results suggest therefore that the decrease in the population of hexameric insulin relative to other oligomers at 70°C is associated with the conversion of soluble insulin to insoluble aggregates.

Characterization of fibrils by electron microscopy, x-ray diffraction, and FT-IR spectroscopy

The morphological changes involved in the formation of insulin fibrils under the conditions of the mass spectrometric experiments were investigated by electron microscopy (EM). The insulin solution before heating did not show appreciable quantities of aggregated material (Fig. 6 *A*). After heating the pH 2.0 solutions containing 2 mM insulin for 3 h at 70°C a network of fibrils is evident, apparently consisting of single protofilaments with a high degree of curvature, indicative of flexibility (Fig. 6 *B*). Continued heating for 48 h shows the development of larger fibrils, many containing at least two protofilaments and having a well-defined helical twist of pitch ~150 Å (Fig. 6 *C*). The fibrils were also analyzed by x-ray fiber diffraction and the resulting diffraction pattern showed a meridional reflection at 4.83 ± 0.01 Å with further reflections at 7.5 ± 0.01 Å and 11.3 ± 0.01 Å (data not shown). These results are consistent with similar data reported previously (Burke and Rougvie, 1972a) and indicate that the fibrils have the characteristic cross-β structure common to all amyloid structures (Sunde et al., 1997).

Fourier transform infrared spectra in the region 1580–1700 cm^{-1} from soluble insulin and two preparations of the aggregated material are shown in Fig. 7. This region contains bands assigned to the amide I modes (essentially C = O stretching vibrations of the amide group) that have been used to characterize the conformation of proteins (Glenner et al., 1974; Wei et al., 1991; Fabian et al., 1993; Vecchio et al., 1996). In the spectrum of insulin in solution at pH 2.0, in which all labile hydrogens were exchanged for deuterium, the peak observed in the amide region has an absorbance maximum at 1648 cm^{-1}. This arises from a convolution of a number of absorption bands corresponding to the various structural elements present in the native solution conformation. In a previous study a peak with an absorption maximum at 1650 cm^{-1} was observed and assigned to a dominant α-helical band (residues B9–B19) (Krimm and Bandekar, 1986). The FT-IR spectra of the samples incubated at 70°C are quite different from that of soluble insulin recorded under the same solution conditions, Fig. 7. The absorbance maximum in the amide region is at 1627 cm^{-1} in the samples incubated for 3 h and 48 h. The contribution to both spectra of the α-helical absorption band in the amide region at 1650 cm^{-1} (Krimm and Bandekar, 1986) is much reduced relative to that of the soluble protein sample. Moreover, this reduction is more marked where the sample has undergone longer incubation. By contrast, the contribution at 1627 cm^{-1}, thought to arise from parallel β-sheet (Wei et al., 1991), increases with the time of sample incubation. These changes are consistent with a substantial reduction in the α-helical content of the protein structure on conversion to amyloid fibrils, accompanied by a corresponding increase in the amount of β-sheet. The persistence of a contribution to the peak at 1650 cm^{-1}, even after the fibrils have been incubated for 48 h, indicates some α-helical and/or unstructured regions remain. However, the predominant structural characteristic of the fibril is its extensive β-sheet nature, a result in accord with data obtained previously (Glenner et al., 1974). In a separate paper we describe the time development of the FT-IR spectrum and its relationship to morphological changes in the EM images (Bouchard et al., submitted).

DISCUSSION

The nature of insulin species under different solution conditions

In the presence of Zn^{2+}, hexamers of insulin containing two to four Zn^{2+} ions have been generated and maintained intact in the gas phase. The insulin species detected in the gas phase correspond closely to those anticipated from earlier solution studies (Lord et al., 1973). The absence of significant intensity for signals from species such as the trimer and pentamer indicates that the dimer, tetramer and hexamer are the stable species under the solution conditions used here. The effect of the concentration of the solutions from which the species are generated has enabled measurements of the stability constants of dimers, tetramers and hexamers to be made. These results show that there is a good agreement between the values of the stability constants obtained from the proportions of species in the gas phase and the values obtained from conventional solution methods (Lord et al., 1973).

At high protein concentration the mass spectra are remarkable in that they show the presence of oligomers containing between 2 and 12 insulin molecules. The relative intensities of the charge states corresponding to the tetramer and the hexamer are higher than those of the pentamer or 7-mer and indicate that the probability of forming even numbered species is higher than forming odd numbered oligomers. The results presented here are consistent with formation of a series of aggregates through association of the dimer to give the tetramer and the hexamer in preference to the pentamer and 7-mer. The relative proportions of the monomeric and higher oligomeric species at 70°C, where rapid fibril formation takes place, show little change in the first hour of incubation. After this time the total solution concentration falls rapidly. The population of all the higher oligomers also decreases relative to the monomer although

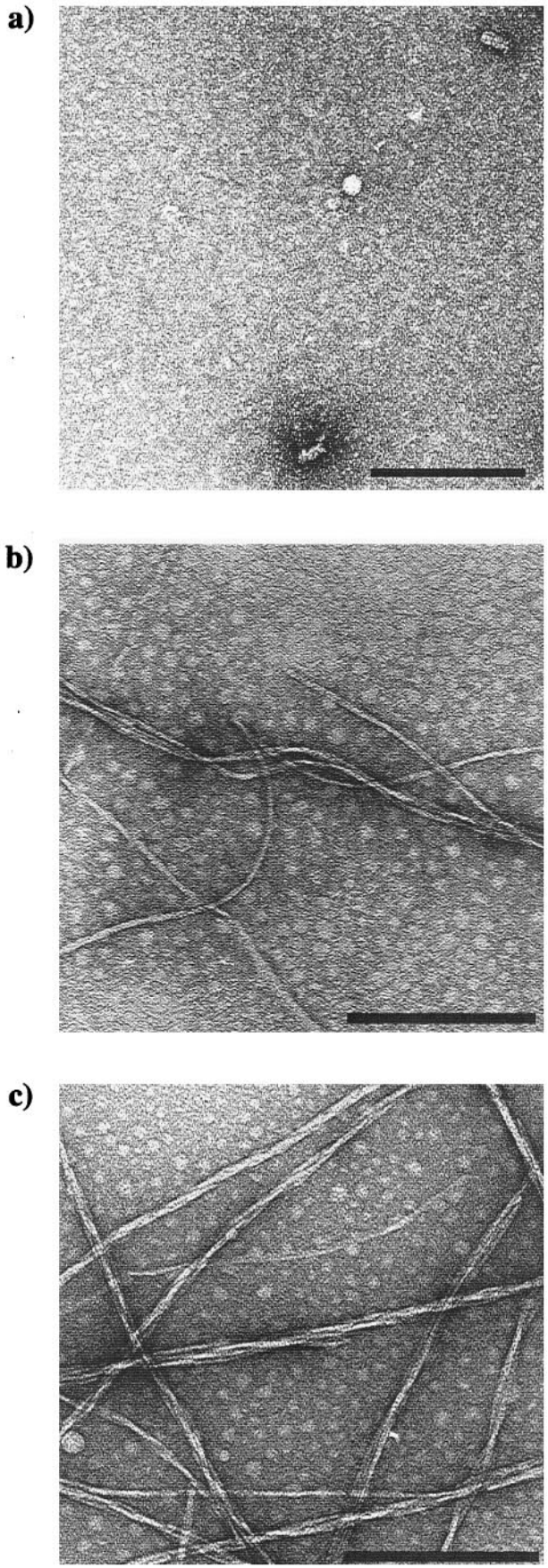

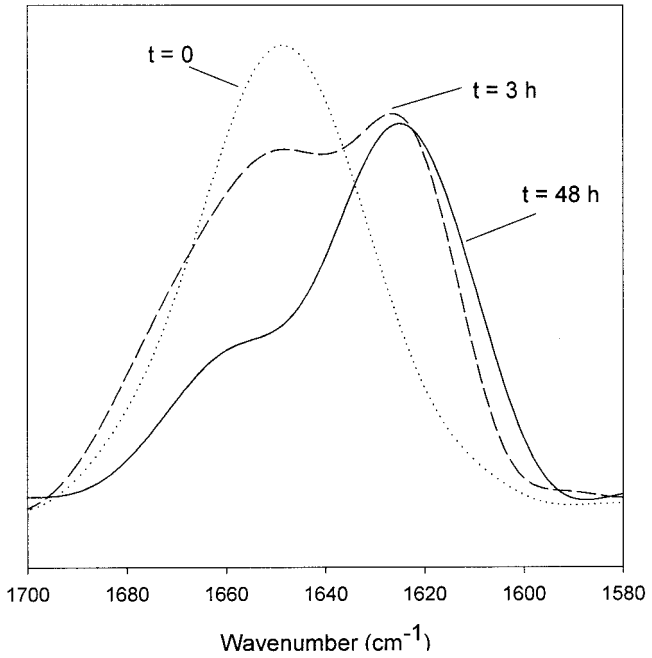

FIGURE 7 FT-IR spectra in the regions 1580–1700 cm^{-1} of soluble insulin and two preparations of fibrils incubated for 3 h and 48 h at 70°C. The spectra show the transition from the essentially α-helical protein before heating to increasing amounts of β-sheet structure during fibril formation.

the intensities of the charge states of the hexamer are reduced to a greater extent than those of the pentamer and tetramer. Spectra recorded for insulin solutions at the same protein pH and concentration but at 60°C, where rapid fibril formation is not observed, did not show such changes in the relative intensities. These results imply that the depletion of the higher oligomers, in particular the hexamer, from the solution at 70°C is connected with the formation of higher aggregates and fibrils rather than to differences in thermal stability of the different oligomers. One possibility is that the hexamer is incorporated into a larger ordered structure during the aggregation process.

Hydrogen exchange measurements reveal that an average of 20 ± 2 hydrogens are protected per insulin molecule in each of oligomeric species examined. This number is similar to that determined from NMR studies of insulin at pH 2.0 in 20% acetic acid, conditions which favor the monomeric form of the protein, where a total of 17 slowly exchanging sites were observed (Hua and Weiss, 1991). The origin of the slightly higher protection against hydrogen

FIGURE 6 Analysis of insulin fibrils by electron microscopy. Electron micrographs of insulin samples were recorded for insulin during fibril formation at 70°C (bar = 2000 Å). Samples were collected before heating (*a*) and after heating for 3 h (*b*), and 48 h (*c*). The micrographs show the transition from young fibrils (*b*) to mature fibrils (*c*) in which the helical twist of at least two protofilaments can be identified.

exchange observed by MS over that recorded by NMR may be attributed to changes in the intrinsic rate of exchange arising from the different solution conditions (Bai et al., 1993). The most important observation from this MS data however is that the higher oligomers do not show increased hydrogen exchange relative to the monomer whereas in stable oligomeric species greater burial of surface area leads to increased protection against exchange (Nettleton, 1998). These results strongly suggest that the rate of interconversion between oligomers is rapid relative to the time scale of the hydrogen exchange measurements allowing solvent molecules to exchange with labile sites in the intermolecular interfaces.

Structural transitions during insulin fibril formation

The results presented here allow us to examine the process of insulin aggregation in the light of the mechanism of fibril formation proposed for other amyloidogenic proteins (Harper and Lansbury, 1997). There is an initial lag phase in the formation of aggregates in which the concentration of soluble insulin is maintained at a level close to its initial value, following the transfer of insulin to conditions under which fibrils eventually form. This phenomenon is seen in other amyloidogenic systems, in particular Aβ 1–40 and Aβ 1–42 exhibit associated with Alzheimer's disease (Jarrett et al., 1993). The lag phase observed in this study is shorter at higher concentrations, 65 $\pm$ 5 min at 2 mM compared with more than 6 h recorded for the 2 μM insulin solution, a finding similar to that observed with Aβ peptides (Jarrett et al., 1993). The absence of very large oligomers (species above 12-mers) is significant given that the time-of-flight instrumentation used for these experiments has recently been shown to be capable of detecting signals from oligomers having masses above 2 MDa (Rostom et al., 2000; Tito et al., 2000). Based on sedimentation properties, high molecular weight oligomers of Aβ 1–40 have been proposed with a molecular weight close to 4 MDa. The present study implies that such species, if formed, are either above 2–3 MDa, or unstable at the high temperature employed to form fibrils or not present at a significant concentration. The oligomers observed for insulin are similar to those reported for transthyretin where a ladder of oligomeric intermediates with increasing molecular weight was observed (Lashuel et al., 1998). The absence of very large intermediates and the presence of a series of oligomers in solutions that ultimately form fibrils may imply that for insulin the nucleation species are relatively small.

The FT-IR spectra and the MS hydrogen exchange measurements of the soluble protein before heating confirm that under the solution conditions used here the various solution species present in the lag phase contain extensive native-like structure. The FT-IR spectra, however, show the emergence of a large signal characteristic of β-sheet structure after the lag phase under conditions in which amyloid fibrils form. The interstrand spacing of 4.83 $\pm$ 0.01 Å measured from x-ray diffraction patterns in the present study is in close agreement with results from other amyloid fibrils (Sunde et al., 1997) showing that the fibrils have the characteristic cross-β-sheet structure found in all other amyloid fibrils. Thus a major structural conversion must occur for insulin on fibril formation, involving substantial unfolding of the molecules to allow conversion of α-helical to β-sheet structure. Destabilization of native state interactions and exposure of the hydrophobic core has been proposed to be involved in conversion of other normally soluble proteins to fibrils. For example hydrogen exchange measurements have shown enhanced conformational dynamics for variants of human lysozyme (Booth et al., 1997; Canet et al., 1999) and transthyretin (Nettleton et al., 1998; Kelly, 1998). The results from the present study of insulin show that substantial loss of native state helical structure or loss of native-like hydrogen exchange protection does not occur during the lag period of fibril formation. Rather the loss of signal from soluble protein, evident in the mass spectra during the lag time, is consistent with the build up of insoluble aggregates which FT-IR shows have extensive helical structure but little β-sheet character.

It appears therefore that there is a dynamic equilibrium involving essentially native–like helical oligomers, present initially during the lag phase, that associate during the latter stages of this phase to form large aggregates. These aggregates, not visible by mass spectrometry, may be related in structure to models proposed for despentapeptide insulin, in which the helical structure of the dimer was used as a model for packing in the fibril (Brange et al., 1997b). The formation of fibrillar structure involves a transition from species with substantial helical structure to those with extensive β-sheet. Although the present study does not provide evidence directly for this step, it must involve a substantial unfolding event in which labile intermolecular interactions are replaced by persistent intramolecular hydrogen bonds either by rearrangement of large aggregates or in a separate nucleation event.

CONCLUSIONS

Despite the widespread use of insulin in the treatment of type I diabetes the incidence of insulin fibril deposits at the site of repeated injection has not been widely reported. This is in contrast to fibril formation by a number of other amyloidogenic proteins associated with clinical disorders. For example β2-microglobulin is always a complication in long term hemodialysis patients (Gejyo et al., 1985) and transthyretin fibrils, associated with both senile and familial forms of systemic amyloidosis, are widespread (Benson, 1989). This could well be due to the relative ease of fibril formation of these proteins from conditions close to those that can exist in vivo. By contrast a number of constraints

exist in the insulin molecule that may give rise to the low incidence of fibrils during the treatment of insulin dependent diabetics. The fact that the native state of insulin is remarkably stable to a wide range of pH and solution conditions and the two short chains are constrained by disulfide bonds suggests that unfolding events will not be favored. This is in contrast to variants of transthyretin and lysozyme where single amino acid mutations compromise their stability leading to higher unfolding rates (Nettleton et al., 1998; Canet et al., 1999) and to β2-microglobulin where a single disulfide bond is present in the 12 kDa protein (Gejyo et al., 1985). In addition, the neutral pH conditions and the intrinsic stability of the Zn^{2+} hexamer used in pharmaceutical preparations of insulin, and the fact that the hexamer does not readily dissociate until the local concentration is below nanomolar, ensure that monomeric insulin does not readily form fibrils. At nanomolar concentration higher oligomers could not be detected by MS and would be unlikely to form in vivo. Interestingly insulin fibril formation has been observed under hydrophobic solution conditions both in vitro (Sluzky et al., 1991) and in vivo after injection using plastic syringes (Dische et al., 1987). Such conditions would be expected to promote unfolding of globular proteins leading to the dissociation of the insulin hexamer at higher local concentrations than in the absence of hydrophobic surfaces, leading to the possibility of aggregation.

In addition to the significance of the present findings for insulin itself, this study demonstrates the utility of mass spectrometry in defining the solution states of a protein system in oligomeric forms. This arises from the unique ability of mass spectrometry to distinguish between chemically identical species with different molecular masses. While the precise quantity of such species is heavily dependent upon the instrumental settings and conditions within the mass spectrometer, the ability to control the dissociation of macromolecular species enables the properties of individual molecules to be defined (Rostom et al., 2000). The proportion of aggregating species detected by mass spectrometry is relatively low in comparison with monomeric species, with the intensity associated with the 12-mer generally being less than 0.1% of the signal for the monomer. The fact that even at this intensity it is possible to detect and probe the persistence of these species during the lag phase of the aggregation process suggests that it might be possible to investigate in more detail species associated with the mechanism of aggregation. Moreover the ability to measure hydrogen exchange properties from a wide range of solution conditions, both individually and as part of a larger assembly, suggests a unique approach to probing the dynamics of association and dissociation processes in complex systems. It seems likely therefore that mass spectrometry can be applied not just to amyloidogenic proteins but to the formation of oligomeric species during aggregation and nucleation processes more generally.

We acknowledge with thanks helpful discussions with Guy Dodson, Jens Brange, and Anne Clark and help with electron microscopy from Emma Jaikaran. This is a contribution from the Oxford Centre for Molecular Sciences, which is funded by the BBSRC, EPSRC, and MRC. E.J.N. and P.T. are grateful for financial support from Glaxo Wellcome and Rhone Poulenc, respectively. M.B. is supported by the Natural Sciences and Engineering Research Council of Canada (NSERC) and by Fonds pour la Formation de Chercheurs et l'Aide à la Recherche (FCAR) of the Province of Québec. M.S. thanks the MRC and Lady Margaret Hall, Oxford. The research of C.M.D. is supported in part by the Wellcome Trust. The research of C.V.R. is supported by the Royal Society.

REFERENCES

Adams, M. J., T. L. Blundell, E. J. Dodson, G. G. Dodson, M. Vijayan, E. N. Baker, M. M. Harding, D. C. Hodgkin, B. Rimmer, and S. Sheat. 1969. Structure of rhombohedral 2 zinc insulin crystal. *Nature.* 224: 491–495.

Bai, Y., J. S. Milne, L. Mayne, and S. W. Englander. 1993. Primary structure effects on peptide group hydrogen exchange. *Proteins Struct. Funct.. Genet.* 17:75–86.

Benson, M. D. 1989. Familial amyloidotic polyneuropathy. *Trends Biochem. Sci.* 12:88–92.

Booth, D., M. Sunde, V. Bellotti, C. V. Robinson, W. L. Hutchinson, P. E. Fraser, P. N. Hawkins, C. M. Dobson, S. E. Radford, C. C. F. Blake, and M. B. Pepys. 1997. Instability, unfolding and aggregation of human lysozyme variants underlying amyloid fibrillogenesis. *Nature.* 385: 787–793.

Bouchard, M., J. Zurdo, E. J. Nettleton, C. V. Robinson, and C. M. Dobson. submitted. Formation of insulin amyloid fibrils followed by FTIR simultaneously with CD and electron microscopy. Submitted.

Brange, J., L. Andersen, E. D. Laursen, G. Meyn, and E. Rasmussen. 1997a:Toward understanding insulin fibrillation. *J. Pharm. Sci.* 86: 517–25.

Brange, J., G. G. Dodson, D. J. Edwards, P. H. Holden, and J. L. Whittingham. 1997b. A model of insulin fibrils derived from the x-ray crystal structure of a monomeric insulin (despentapeptide insulin). *Proteins Struct. Funct. Genet.* 27:507–16.

Brange, J., J. Whittingham, D. Edwards, Y.-S. Zhang, A. Wollmer, D. Brandenburg, G. Dodson, and J. Finch. 1997c. Insulin structure and diabetes treatment. *Curr. Sci.* 72:470–476.

Brange, J., and A. Volund. 1999. Insulin analogs with improved pharmacokinetic profiles. *Adv. Drug Delivery Revs.* 35:307–335.

Burke, M. J., and M. A. Rougvie. 1972a. Cross-protein structures. I. Insulin fibrils. *Biochemistry.* 11:2435–9.

Burke, M. J., and M. A. Rougvie. 1972b. Cross-protein structures. I. Insulin fibrils. *Biochemistry.* 11:2435–9.

Canet, D., M. Sunde, A. M. Last, A. Miranker, A. Spencer, C. V. Robinson, and C. M. Dobson. 1999. Mechanistic studies of the folding of human lysozyme and the origin of amyloidogenic behavior in its disease related variants. *Biochemistry.* 38:6419–6427.

Dische, F. E., C. Wernstedt, G. T. Westermark, P. Westermark, M. B. Pepys, S. G. Gilbey, and P. J. Watkins. 1987. Localized deposition of an insulin-containing amyloid in a diabetic at sites of repeated injections of porcine insulin. *J. Pathol.* 152:A194–A194.

Fabian, H., L. P. Choo, G. I. Szendrei, M. Jackson, W. C. Halliday, L. Otvos, and H. H. Mantsch. 1993. Infrared spectroscopic characterization of Alzheimer plaques. *Appl. Spectrosc.* 47:1513–1518.

Fabris, D., and C. Fenneslau. 1999. Characterization of allosteric insulin hexamers by electrospray ionization mass spectrometry. *Anal. Chem.* 71:384–387.

Gejyo, F., T. Yamada, S. Odani, Y. Nakagawa, M. Arakawa, T. Kunitomo, H. Kataoka, M. Suzuki, Y. Hirasawa, T. Shirahama, A. S. Cohen, and K. Schmid. 1985. A new form of amyloid protein associated with hemodialysis was identified as b2-microglobulin. *Biochem. Biophys. Res. Commun.* 129:701–706.

Glenner, G. G., E. D. Eanes, H. A. Bladen, R. P. Linke, and J. D. Termine. 1974. Beta-pleated sheet fibrils: a comparison of native amyloid with synthetic protein fibrils. *J. Histochem. Cytochem.* 22:1141–58.

Goldman, J., and F. H. Carpenter. 1974. Zinc binding, circular dichroism, and equilibrium sedimentation studies on insulin (bovine) and several of its derivatives. *Biochemistry.* 13:4566–4574.

Harper, J. T., and P. T. Lansbury. 1997. Models of amyloid seeding in Alzheimer's disease and scrapie: mechanistic truths and physiological consequences of the time dependent solubility of amyloid proteins. *Annu. Rev. Biochem.* 66:385–407.

Hua, Q. X., and M. A. Weiss. 1991. Comparative 2D-NMR studies of human insulin and des-pentapeptide insulin—sequential resonance assignment and implications for protein dynamics and receptor recognition. *Biochemistry.* 30:5505–5515.

Jarrett, J. T., E. P. Berger, and P. T. Lansbury. 1993. *Ann. NY Acad. Sci.* 695:870–877.

Jeffrey, P. D., and J. H. Coates. 1966. An equilibrium ultracentrifuge study of the self-association of bovine insulin. *Biochemistry.* 5:489–498.

Kelly, J. W. 1998. The alternative conformations of amyloidogenic proteins and their multi-step assembly pathways. *Curr. Opin. Struct. Biol.* 8:101–106.

Koltun, W. L., D. F. Waugh, and R. S. Bear. 1954. An x-ray diffraction investigation of selected types of insulin fibrils. *J. Am. Chem. Soc.* 76:413–417.

Krimm, S., and J. Bandekar. 1986. Vibrational spectroscopy and conformation of peptides, polypeptides, and proteins. *Adv. Protein Chem.* 38:181–364.

Kuster, B., and M. Mann. 1998. Identifying proteins and post-translational modifications by mass spectrometry. *Curr. Opin. Struct. Biol.* 8:393–400.

Langmuir, I., and D. F. Waugh. 1940. Pressure-soluble and pressure-displaceable components of monolayers of native and denatured proteins. *J. Am. Chem. Soc.* 62:2771–2793.

Lashuel, H. A., Z. Lai, and J. W. Kelly. 1998. Characterization of the transthyretin acid denaturation pathways by analytical ultracentrifugation: implications for wild-type, V30M, and L55P amyloid fibril formation. *Biochemistry.* 37:17851–17864.

Lord, R. S., F. Gubensek, and J. A. Rupley. 1973. Insulin self-association. *Spectrum Changes Thermodyn. Biochem.* 12:4385–4392.

Mirza, U. A., and B. T. Chait. 1994. Effects of anion on the positive ion electrospray ionization mass spectra of peptides and proteins. *Anal. Chem.* 66:2898–2904.

Nettleton, E. J. 1998. Ph.D. thesis, Oxford University.

Nettleton, E. J., M. Sunde, V. Lai, J. W. Kelly, C. M. Dobson, and C. V. Robinson. 1998. Protein subunit interactions and structural integrity of amyloidogenic transthyretins: evidence from electrospray mass spectrometry. *J. Mol. Biol.* 281:553–564.

Pocker, Y., and S. B. Biswas. 1981. Self-association of insulin and the role of hydrophobic bonding: a thermodynamic model of insulin dimerization. *Biochemistry.* 20:4354–4361.

Rostom, A. A., P. Fucini, D. R. Benjamin, R. Juenemann, K. H. Nierhaus, F. U. Hartl, C. M. Dobson, and C. V. Robinson. Selective dissociation of intact ribosomes in a mass spectrometer. *Proc. Natl. Acad. Sci. USA.* 97:5185–5190.

Rostom, A. A., and C. V. Robinson. 1999. Disassembly of macromolecular complexes in the gas phase. *Curr. Opin. Struct. Biol.* 9:135–141.

Schlichtkrull, J. 1958. Insulin Crystals. Munksgaard, Copenhagen.

Sluzky, V., J. A. Tamada, A. M. Klibaonov, and R. Langer. 1991. Kinetics of insulin aggregation in aqueous solutions upon agitation in the presence of hydrophobic surfaces. *Proc. Natl. Acad. Sci. USA.* 88: 9377–9381.

Smith, G. D., D. C. Swenson, E. J. Dodson, G. G. Dodson, and C. D. Reynolds. 1984. Structural stability in the 4-zinc human insulin hexamer. *Proc. Natl. Acad. Sci. USA.* 81:7093–7097.

Sunde, M., L. C. Serpell, M. Bartlam, P. E. Fraser, M. B. Pepys, and C. C. F. Blake. 1997. Common core structure of amyloid fibrils by synchrotron x-ray diffraction. *J. Mol. Biol.* 273:729–739.

Tito, M. A., K. Tars, K. Valegard, J. Hadju, and C. V. Robinson. Electrospray time-of-flight mass spectrometry of the intact MS2 virus capsid. *J. Am. Chem. Soc.* 122:350–351.

Vecchio, G., A. Bossi, P. Pasta, and G. Carrea. 1996. Fourier-transform infrared conformational study of bovine insulin in surfactant solutions. *Int. J. Pep. Prot. Res.* 48:113–117.

Vis, H., U. Heinemann, C. M. Dobson, and C. V. Robinson. 1998. Detection of a monomeric intermediate associated with dimerization of protein HU by mass spectrometry. *J. Am. Chem. Soc.* 120:6427–6428.

Waugh, D. F., D. F. Wilhelmson, S. L. Commerford, and M. L. Sackler. 1957. A mechanism for the formation of fibrils from protein molecules. *J. Cell. Comp. Physiol.* 49:145–164.

Wei, J., Y. Z. Lin, J. M. Zhou, and C. L. Tsou. 1991. FT-IR studies of secondary structures of bovine insulin and its derivatives. *Biochim. Biophys. Acta.* 1080:29–33.

Wilm, M., and M. Mann. 1994. Electrospray and Taylor- one theory: Dole's beam of macromolecules at last? *Int. J. Mass Spectrom. Ion Proc.* 136:167–180.